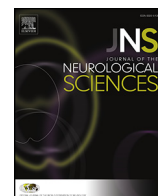




Contents lists available at ScienceDirect

Journal of the Neurological Sciences

journal homepage: [www.elsevier.com/locate/jns](http://www.elsevier.com/locate/jns)

## Gait characteristics in a canine model of X-linked myotubular myopathy

Melissa A. Goddard<sup>a</sup>, Emily Burlingame<sup>b</sup>, Alan H. Beggs<sup>c</sup>, Anna Buj-Bello<sup>d</sup>, Martin K. Childers<sup>e,f</sup>, Anthony P. Marsh<sup>b</sup>, Valerie E. Kelly<sup>e,\*</sup>

<sup>a</sup> Department of Physiology and Pharmacology, School of Medicine, Wake Forest University, Winston-Salem, NC 27109, USA

<sup>b</sup> Department of Health and Exercise Science, Wake Forest University, Winston-Salem, NC 27109, USA

<sup>c</sup> Division of Genetics and Genomics, The Manton Center for Orphan Disease Research, Boston Children's Hospital, Harvard Medical School, Boston, MA 02115, USA

<sup>d</sup> Généthon, 1 bis rue de l'Internationale, 91002 Evry, France

<sup>e</sup> Department of Rehabilitation Medicine, School of Medicine, University of Washington, Seattle, WA 98195, USA

<sup>f</sup> Institute for Stem Cell and Regenerative Medicine, University of Washington, Seattle, WA 98109, USA

### ARTICLE INFO

#### Article history:

Received 11 February 2014

In received in revised form 22 July 2014

Accepted 22 August 2014

Available online xxx

#### Keywords:

Myotubular myopathy

Locomotion

Gait

Animal models

Biomechanics

Kinematics

### ABSTRACT

X-linked myotubular myopathy (XLMTM) is a fatal pediatric disease where affected boys display profound weakness of the skeletal muscles. Possible therapies are under development but robust outcome measures in animal models are required for effective translation to human patients. We established a naturally-occurring canine model, where XLMTM dogs display clinical symptoms similar to those observed in humans. The aim of this study was to determine potential endpoints for the assessment of future treatments in this model. Video-based gait analysis was selected, as it is a well-established method of assessing limb function in neuromuscular disease and measures have been correlated to the patient's quality of life. XLMTM dogs (N = 3) and their true littermate wild type controls (N = 3) were assessed at 4–5 time points, beginning at 10 weeks and continuing through 17 weeks. Motion capture and an instrumented carpet were used separately to evaluate spatiotemporal and kinematic changes over time. XLMTM dogs walk more slowly and with shorter stride lengths than wild type dogs, and these differences became greater over time. However, there was no clear difference in angular measures between affected and unaffected dogs. These data demonstrate that spatiotemporal parameters capture functional changes in gait in an XLMTM canine model and support their utility in future therapeutic trials.

© 2014 Elsevier B.V. All rights reserved.

### 1. Introduction

X-linked myotubular myopathy (XLMTM) is a fatal inherited disease of the skeletal muscle, estimated to affect 1 in every 50,000 male births [1]. Patients typically present with hypotonia, generalized muscle weakness and respiratory failure at birth [2]. Survival beyond the postnatal period requires intensive support, often including gastrostomy feeding and mechanical ventilation [3,4]. The disease negatively impacts the quality of life of affected children and requires intensive support from caregivers. XLMTM is caused by the absence of the phosphoinositide phosphatase myotubularin due to mutation of the *MTM1* gene on the long arm of the X chromosome [5]. There is no cure for XLMTM and current treatment options are primarily palliative. Prospective approaches in therapy therefore target the replacement of the gene or the gene product [6,7], an approach referred to as gene replacement therapy or gene transfer therapy.

**Abbreviations:** XLMTM, X-linked myotubular myopathy; AAV8, serotype-8 adeno-associated virus.

\* Corresponding author at: 1959 NE Pacific Street, Box 356490, Seattle, WA 98195-6490, USA. Tel.: +1 206 598 5350.

E-mail address: [vekelly@u.washington.edu](mailto:vekelly@u.washington.edu) (V.E. Kelly).

The development of animal models of XLMTM, such as in mice and zebrafish, has been a crucial step in the process of understanding the disease pathogenesis and developing potential therapies [8,9]. Indeed, adeno-associated virus (AAV)-mediated gene replacement therapy has produced promising results in the mouse model [7,10]. However, these are limited systems for translation into human patients, particularly when assessing restoration of function. Due to its size, a larger animal model, like the dog, more closely approximates the clinical condition in human neuromuscular disorders [11]. Also, the ability of the large animal model to tolerate repeated measurements allows for a longitudinal investigation that can more powerfully inform studies of efficacy.

A colony of XLMTM dogs descended from a Labrador Retriever carrier female with a naturally occurring missense mutation was recently established [12]. Affected male dogs appear similar to male patients, displaying not only severe muscle weakness [13] but also many of the classic features of the disease, such as a narrow head-shape and long, thin limbs [4]. XLMTM dogs decline rapidly, with a maximal lifespan of around 5 months of age and a failure to thrive analogous to the human disease. We recently reported that intravenous administration of a single dose of a recombinant serotype-8 adeno-associated virus (AAV8) vector expressing canine myotubularin to *MTM1*-deficient

<http://dx.doi.org/10.1016/j.jns.2014.08.032>

0022-510X/© 2014 Elsevier B.V. All rights reserved.

Please cite this article as: Goddard MA, et al, Gait characteristics in a canine model of X-linked myotubular myopathy, J Neurol Sci (2014), <http://dx.doi.org/10.1016/j.jns.2014.08.032>

dogs resulted in robust improvement in motor activity and contractile force, corrected muscle pathology and prolonged survival [10].

As gene therapy or other interventions are developed and tested in the XLMTM canine model, methods for evaluating potential changes in motor function are crucial as predictors of quality of life [14]. Therefore analogs of such clinical tests are particularly powerful when determining the outcome of gene therapy trials. Changes in ambulation have been well established in the literature as indicators of functional loss in human patients [15–17]. Parameters such as gait velocity and stride length, as well as sagittal plane measurement of hip, knee and ankle joints have been used as functional outcome measures [18]. Such systems have been adapted for use in canine models of neuromuscular diseases. For example, in the golden retriever muscular dystrophy (GRMD) dog, video-based gait assessment can capture not only spatiotemporal changes due to the presence of disease, such as reduced speed, but also kinematic accommodations, such as changes in hock or stifle angles [19]. We therefore propose that similar spatiotemporal or kinematic changes in gait can be used as quantitative outcome measures in the canine XLMTM model. Here we report a case series of XLMTM and wild type dogs in which video-based gait analysis was used to assess differences in gait over time.

## 2. Methods

This was an early-stage observational study designed to examine possible differences in gait characteristics among experimental and wild type control groups. Spatiotemporal gait parameters were assessed using both video-based motion capture and an instrumented carpet, and kinematic gait parameters were assessed with video-based motion capture.

### 2.1. Dogs

Use and care of animals followed principles outlined in the National Institutes of Health Guide for the Care and Use of Laboratory Animals. Affected XLMTM dogs from two litters were identified just after birth by Taqman genotyping assay, as previously described [12]. XLMTM dogs ( $N = 3$ ) and their true littermate controls ( $N = 3$ ) were then assessed at 4–5 time points, beginning at 10 weeks and continuing through 17 weeks for litter A and 15 weeks for litter B. The cranial tibialis muscle of the left hind limb of affected dogs was injected at 10 weeks of age with AAV8-*cMTM1* ( $4 \times 10^{11}$  viral genomes) diluted in 1 mL lactated Ringer's solution, as described previously [10]. At the same time, the cranial tibialis muscle of the right hind limb of affected

dogs was injected with an equal volume of Ringer's solution alone. Unaffected littermate controls received 1 mL of Ringer's solution in each hind limb. We did not anticipate local intramuscular injection of this muscle to impact walking, as this muscle is a flexor of the hind limb.

### 2.2. Motion capture

#### 2.2.1. Filming

Quantitative gait analysis was carried out using 2-dimensional video-based motion capture to assess kinematic and spatiotemporal aspects of gait, as previously demonstrated in a canine model of muscular dystrophy [19]. Retro-reflective tape was placed on the greater trochanter of the femur, a point equidistant between the lateral epicondyle of the femur and the fibular head, the lateral malleolus of the distal tibia, and the distolateral aspect of the fifth metatarsus (Fig. 1).

Dogs were filmed walking at a self-selected pace against a dark cloth backdrop and across a black mat, with motion capture data recorded in the middle 2.4 m and instrumented carpet data recorded over the middle 4.9 m of the walkway to ensure a steady gait speed. A premeasured distance of 1.5 m was also marked on the mat for later video trial selection. A leash, food reward or vocal encouragement was used with both normal and affected animals. The dogs were walked left-to-right and right-to-left to film the left and right sides using a single camera operating at 60 Hz (DCR-SX63, Sony, Japan). The camera was leveled and zoomed to encompass the filming volume and camera exposure was adjusted and a spotlight was used for optimal brightness of the reflective markers.

#### 2.2.2. Processing

All videos for a single dog at a given time point were first sorted for quality based on the consistency of both speed and gait patterns, the position of the head (up and pointing forward), and the straightness of the walk through the filming volume. Trials where the dog walked out of the volume or abruptly changed gait pattern or speed were discarded. The remaining trials were independently reviewed and scored on a 1 (best)–5 (worst) scale by investigators with experience observing canine gait. The investigator scores for a given trial were averaged. To assess speed, the time for each dog to walk a premeasured distance of 150 cm was recorded by an investigator using a stop watch. For both the right and left sides, the two best video trails based on quality score and similarity of speed were identified for kinematic analysis.

We processed selected video trials using MaxTRAQ software (standard version 2.2.4.2), including calibration of distance for each trial and digitization of each retro-reflective marker on a frame-by-frame

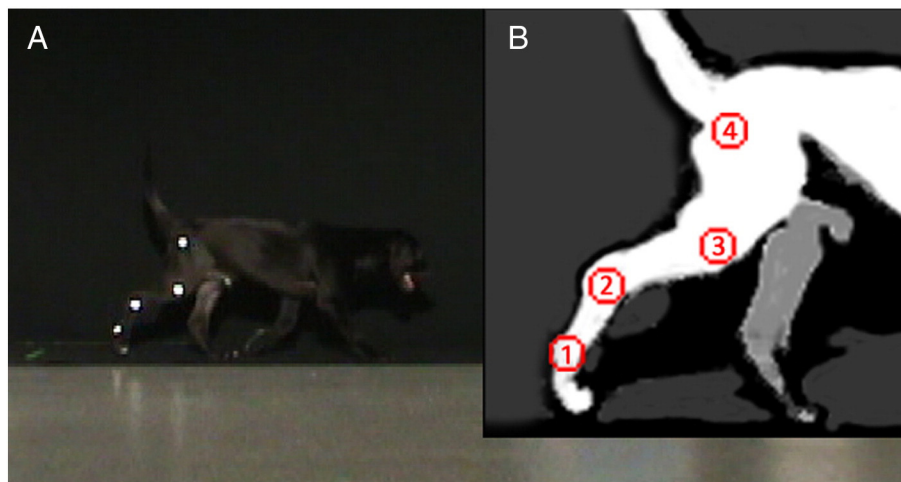


**Fig. 1.** (A) Normal dog on carpet with reflective markings. (B) Reflective markers placed at (1) the distolateral aspect of the paw, (2) the lateral malleolus of the fibula, (3) a point equidistant between the lateral epicondyle of the femur and the greater trochanter, and (4) the greater trochanter of femur.

basis. Data were exported to Visual 3D (C-Motion, Inc., Germantown, USA) for calculation of both spatiotemporal and kinematic measures. Raw 2-dimensional marker coordinates were filtered using a 2nd order Butterworth filter with a cutoff frequency of 4 Hz. Heel-strike and toe-off events were identified for each trial in order to calculate stride and step parameters.

### 2.2.3. Spatiotemporal and kinematic measures

Spatiotemporal measures assessed in this study included stride velocity, stride length, stride time, stance time, and swing time. Stride length was calculated as the excursion of the marker on the fifth metatarsus from one heel strike to the next heel strike on the same leg. Stride time was calculated as the time from one heel strike to the next heel strike on the same leg. Stride velocity was defined as stride length divided by stride time. Stance time referred to the time when the measured hindlimb was in contact with the ground, calculated as the time from heel strike to the following toe off. Swing time referred to the time when the limb was moving forward, calculated from toe off to the following heel strike. Kinematic analyses focused on the stifle and hock joints, with sagittal plane joint angles calculated as previously described [19]. Maximum and minimum angles were determined and used to calculate the joint excursion for each stride.

### 2.3. Instrumented carpet

An instrumented carpet (GAITrite Electronic Walkway, CIR Systems Inc.) measuring  $0.9 \times 7$  m was also used to collect spatiotemporal measures, as previously demonstrated in healthy canines [20]. Instrumented carpet data were collected one week prior to the final time point ( $T_F - 1$ ) and again at the final time point of the experiment ( $T_F$ ). Note that these were separate sessions from those in which motion capture data was collected. Dogs were walked at a self-selected pace across the carpet. Specialized software (GAITFour version 4.1, CIR Systems Inc.) designed to analyze quadrupedal gait was used to quantify velocity calculated as the distance walked across the carpet divided by the time required to do so. Walks across the gait carpet were selected based on the criteria described above.

### 2.4. Statistical analysis

Descriptive analyses were used to summarize physical characteristics and gait parameters for the XLMTM and wild type groups (IBM SPSS Statistics version 19.0, Armonk, USA). Although the power to detect a significant difference is low with such a small sample size, non-parametric tests were used in addition to descriptive analyses to assess differences in gait parameters between groups. Non-parametric Mann–Whitney U tests were used to assess group differences in spatiotemporal and kinematic gait parameters at 10 weeks of age ( $T_0$ ) and at the final time point of 17 weeks of age for litter A and 15 weeks for litter B ( $T_F$ ). Significance for all tests was set at  $\alpha \leq 0.05$ .

## 3. Results

### 3.1. Dogs

Table 1 shows the descriptive characteristics for XLMTM and wild type dogs. Mean (standard deviation) body mass was 7.2 (2.8) at  $T_0$  and 13.7 (4.6) kg at  $T_F$  for wild type dogs and 6.6 (0.7) at  $T_0$  and 9.8 (0.8) kg at  $T_F$  for XLMTM dogs. Mean hind limb length was 24.7 (0.2) at  $T_0$  and 31.1 (2.1) cm at  $T_F$  for wild type dogs and 23.5 (1.6) at  $T_0$  and 30.2 (0.4) cm at  $T_F$  for XLMTM dogs. Body mass and hind limb length did not differ between groups at either time point. Most of the dogs tested were males, except for litter B where no suitable male control was available.

**Table 1**

Descriptive characteristics for the affected XLMTM dogs and their wildtype littermates, where  $T_0$  is at 10 weeks of age and  $T_F$  is the final time point of 17 weeks of age for litter A and 15 weeks for litter B.

Dog	Sex	Age (weeks)	Body mass (kg)		Hind limb length (cm)	
			$T_0$	$T_F$	$T_0$	$T_F$
<i>Litter A</i>						
WT <sub>A1</sub>	M	17	9.0	16.4	24.8	33.3
WT <sub>A2</sub>	M	17	8.6	16.2	24.7	30.9
XLMTM <sub>A1</sub>	M	17	7.2	10.0	22.0	30.5
XLMTM <sub>A2</sub>	M	17	6.8	10.4	23.3	30.2
<i>Litter B</i>						
WT <sub>B1</sub>	F	15	3.9	8.4	24.5	29.1
XLMTM <sub>B1</sub>	M	15	5.8	8.9	25.1	29.8

### 3.2. Spatiotemporal data

#### 3.2.1. Motion capture data

No differences in stride velocity, stride length, stride time, stance time, or swing time were detected between the left and right sides. Therefore, data from the right and left sides were combined for these spatiotemporal measures. In general, XLMTM dogs walked slower than their wild type littermates, and differences in gait speed between the groups became more pronounced over time (Fig. 2). At  $T_0$ , the average stride velocity of XLMTM dogs was 13% less than the velocity measured in wild type animals, though this was not statistically significant ( $p = 0.13$ ). By the final time point, XLMTM dogs walked more slowly than wild type controls ( $p = 0.05$ ), with gait speed in XLMTM dogs 46% lower at  $T_F$  than that in wild type littermate controls.

Stride lengths of XLMTM dogs were shorter than their wild type littermates at both  $T_0$  and  $T_F$  (both  $p = 0.05$ ). The stride length of XLMTM was 86% and 68% that of wild type dogs at 10 weeks of age and the final time point, respectively (Fig. 3).

Stride time and swing time appeared to be similar between groups and over time, but XLMTM dogs demonstrated 65% longer stance times than wild type dogs by the final time point ( $p = 0.05$ ; Table 2).

#### 3.2.2. Instrumented carpet data

Similar to the motion capture data, analysis using the instrumented carpet showed that velocity in the XLMTM dogs was 60% of wild type dogs at  $T_F - 1$  and decreased over time to 50% of the wild type velocity one week later at  $T_F$  (Fig. 4).

### 3.3. Kinematic data

The maximal, minimal and excursion values of the left and right hock (Table 3) and stifle (Table 4) joint angles were analyzed for both

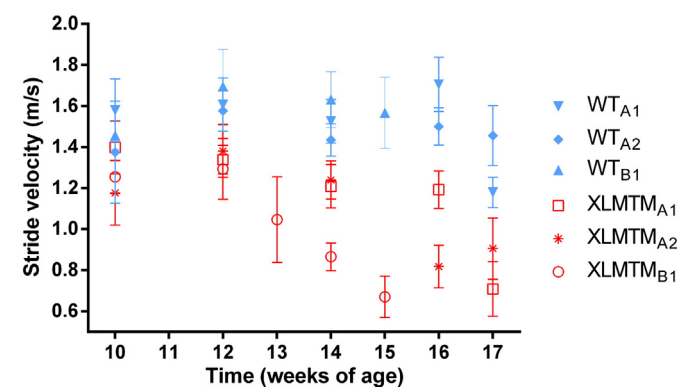


**Fig. 2.** Stride velocities over time for affected XLMTM dogs and their wild type littermates. Symbols represent means and bars represent standard deviations of all trials collected at a given time point.



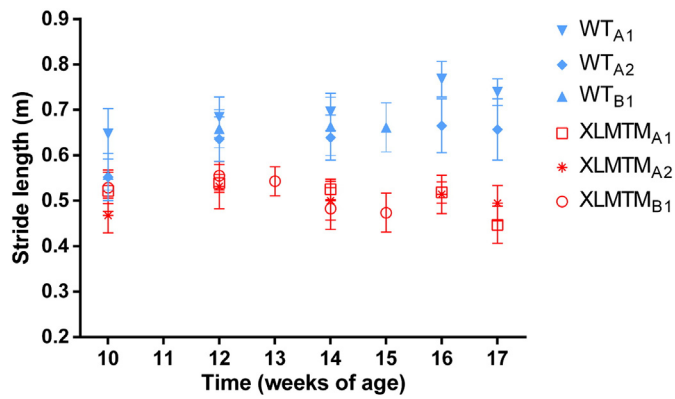


**Fig. 3.** Stride length over time for affected XLMTM dogs and their wild type littermates. Symbols represent means and bars represent standard deviations of all trials collected at a given time point.

groups (see supplementary materials for individual dog data). Maximal, minimal, and excursion joint angle values were consistent between the left and right sides for both the hock and stifle. No differences in hock or stifle kinematics were detected between XLMTM and wild type dogs (all  $p > 0.05$ ).

**4. Discussion**

The main finding from this observational gait study is that compared to normal littermate controls, XLMTM dogs walk more slowly and with shorter stride lengths than wild type dogs. These differences become greater as the disease progresses. The reduced velocity seen in affected animals appears to be characterized by shorter steps and a longer stance phase. Hock and stifle kinematics did not differ between XLMTM and wild type dogs, suggesting that spatiotemporal parameters were more

**Table 2**  
Spatiotemporal data as measured by motion capture for the affected animals and their wildtype littermates, where  $T_0$  is at 10 weeks of age,  $T_1$  is at 12 weeks of age and  $T_F$  is the final time point of 17 weeks of age for litter A and 15 weeks for litter B.

Spatiotemporal data			
	$T_0$	$T_1$	$T_F$
Stride velocity (m/s)			
<i>XLMTM</i>			
mean (SD)	1.28 (0.11)	1.34 (0.04)	0.76 (0.13)
<i>Wild type</i>			
mean (SD)	1.47 (0.10)	1.62 (0.06)	1.40 (0.20)
Stride length (m)			
<i>XLMTM</i>			
mean (SD)	0.51 (0.03)	0.54 (0.01)	0.47 (0.02)
<i>Wild type</i>			
mean (SD)	0.59 (0.05)	0.66 (0.02)	0.69 (0.05)
Stride time (s)			
<i>XLMTM</i>			
mean (SD)	0.40 (0.02)	0.41 (0.02)	0.64 (0.08)
<i>Wild type</i>			
mean (SD)	0.40 (0.02)	0.41 (0.02)	0.50 (0.11)
Stance time (s)			
<i>XLMTM</i>			
mean (SD)	0.21 (0.02)	0.22 (0.01)	0.41 (0.06)
<i>Wild type</i>			
mean (SD)	0.21 (0.01)	0.21 (0.02)	0.25 (0.05)
Swing time (s)			
<i>XLMTM</i>			
mean (SD)	0.19 (0.01)	0.19 (0.01)	0.23 (0.02)
<i>Wild type</i>			
mean (SD)	0.19 (0.01)	0.20 (0.01)	0.22 (0.01)

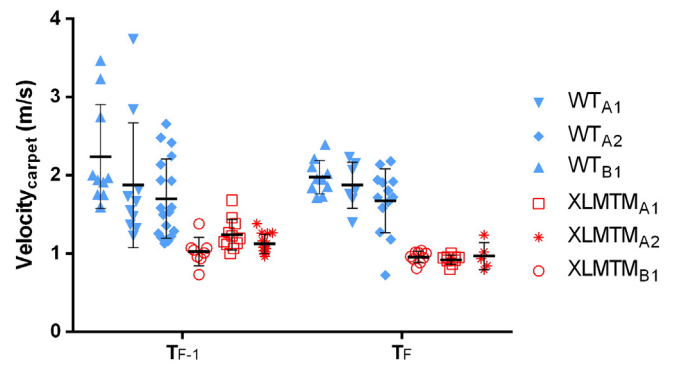


**Fig. 4.** Velocity as measured by the instrumented carpet for affected XLMTM dogs and their wildtype littermates, measured one week prior to the end of the experiment ( $T_F-1$ ) and at the final time point ( $T_F$ ). Each point represents the velocity measured during a single walking trial across the instrumented carpet. Black symbols represent means and bars represent standard deviations for each time point.

sensitive to differences between groups than kinematic parameters. We previously reported progressive limb muscle weakness in XLMTM dogs over time [21], and findings reported here suggest that decreases in gait velocity are a significant functional consequence of this progressive weakness. Taken together, these observations suggest that muscular weakness observed in XLMTM dogs may be an important underlying impairment that leads to slower gait. Our data also indicate that spatiotemporal parameters can distinguish between affected and unaffected dogs and, importantly for future studies of therapy, are sensitive to change over time.

An exemplar outcome measure for clinical translation should reflect a meaningful activity of daily living. The International Classification of Functioning, Disability, and Health: Children and Youth Version calls for outcome measures to address not only limb muscle strength but also relevant functional tasks [22], and recent research promotes this framework to inform the choice of outcome measures for boys with Duchenne muscular dystrophy [23]. Gait measures are functionally meaningful and, particularly in the context of animal models, offer the benefit of being assessed in awake, behaving animals. While we have previously published measures of limb strength in the XLMTM canine model [13], this is the first report of the associated decline in associated limb function, reflected by slower gait speed in the XLMTM compared to wild type dogs. In boys with Duchenne muscular dystrophy, gait speed is correlated with reduced participation in daily life [23] and quality of life [24,25], supporting functional relevance of gait assessments. Indeed, gait speed is widely used as an outcome measure in clinical trials for muscular dystrophy [26–35]. Gait abnormalities have also been reported in canines with Duchenne muscular dystrophy and other myopathies [19,27,36–40]. Some measures of muscle strength and respiratory function have already been reported in the XLMTM dog [13,41], but this is the first study of gait assessment in this large animal model and the first assessment of awake animals.

We recently reported the effects of local intramuscular delivery of AAV8 expressing MTM1 to the cranial tibialis muscle in the three XLMTM dogs also described here. The left hindlimb was injected with AAV8 and the right limb was injected with saline. In that study, we observed marked increase in the strength of the muscle receiving gene replacement therapy, the cranial tibialis (a flexor of the hind limb). We did not detect strength changes in the extensor muscles of the hindlimb, nor did we observe other histopathological changes in any other muscles, indicating a local effect of the test article with this method of administration. Because the cranial tibialis muscle is a flexor of the paw (e.g. muscle contraction lifts the paw up off the ground during gait), local strength changes in this muscle may be insufficient to cause detectable changes in measures of gait [15]. In support of this, we did not detect differences between the right and left sides in spatiotemporal or kinematic measures due to local effects of AAV8 in XLMTM

**Table 3**Hock joint angular data as measured by motion capture, where T<sub>0</sub>, T<sub>1</sub> and T<sub>F</sub> are as described in Table 2, for the affected animals and their wild type littermates.

Hock joint angular data							
	T <sub>0</sub>		T <sub>1</sub>		T <sub>F</sub>		
	L	R	L	R	L	R	
Maximum (°)							
<i>XLMTM</i>	158.6	153.9	147.2	150.9	146.8	145.1	
mean (SD)	(8.4)	(4.4)	(3.4)	(4.6)	(5.8)	(2.6)	
<i>Wildtype</i>	144.0	145.9	146.8	148.4	153.0	154.3	
mean (SD)	(7.3)	(4.6)	(2.6)	(12.9)	(6.5)	(7.8)	
Minimum (°)							
<i>XLMTM</i>	121.9	115.3	111.5	113.8	109.2	118.7	
mean (SD)	(9.6)	(12.6)	(5.3)	(7.0)	(2.8)	(1.0)	
<i>Wildtype</i>	107.4	103.4	109.0	109.7	113.2	118.6	
mean (SD)	(14.2)	(8.7)	(6.5)	(17.2)	(6.5)	(5.2)	
Excursion (°)							
<i>XLMTM</i>	36.7	38.6	35.7	37.1	37.6	26.4	
mean (SD)	(1.9)	(9.4)	(2.1)	(6.5)	(4.4)	(3.6)	
<i>Wildtype</i>	36.6	42.5	37.8	38.7	39.7	35.7	
mean (SD)	(10.1)	(4.6)	(7.5)	(4.3)	(4.4)	(4.5)	

**Table 4**Stifle joint angular data as measured by motion capture, where T<sub>0</sub>, T<sub>1</sub> and T<sub>F</sub> are as described in Table 2, for the affected animals and their wild type littermates.

Stifle joint angular data							
	T <sub>0</sub>		T <sub>1</sub>		T <sub>F</sub>		
	L	R	L	R	L	R	
Maximum (°)							
<i>XLMTM</i>	151.8	143.8	142.4	133.2	142.3	141.8	
mean (SD)	(2.8)	(8.2)	(5.1)	(9.7)	(3.1)	(10.5)	
<i>Wildtype</i>	148.9	147.4	140.8	142.1	145.4	142.7	
mean (SD)	(4.5)	(6.8)	(13.1)	(11.2)	(2.6)	(4.6)	
Minimum (°)							
<i>XLMTM</i>	109.0	102.9	107.0	97.4	109.9	110.0	
mean (SD)	(5.1)	(9.8)	(5.0)	(9.0)	(0.5)	(4.4)	
<i>Wildtype</i>	103.0	99.6	98.6	99.5	109.7	105.6	
mean (SD)	(13.6)	(12.5)	(19.8)	(11.5)	(4.0)	(9.4)	
Excursion (°)							
<i>XLMTM</i>	42.9	40.9	35.3	35.8	32.4	31.7	
mean (SD)	(2.4)	(4.0)	(0.2)	(4.2)	(3.3)	(6.1)	
<i>Wildtype</i>	45.9	47.8	42.2	42.6	35.8	37.1	
mean (SD)	(9.2)	(6.7)	(6.7)	(3.1)	(2.4)	(5.0)	

dogs. However additional studies evaluating systemic effects of AAV8-mediated MTM1 gene replacement on gait in this model are underway. While children with XLMTM are not typically ambulatory, understanding the effects of such therapies in canine models on functionally relevant tasks like walking as well as the effects on respiratory muscle function and limb muscle strength further justifies the development of these therapies.

The current study demonstrates that both motion capture and instrumented carpet methodologies can be used to quantify differences in spatiotemporal parameters between XLMTM and wild type dogs. Given the similarities between motion capture and instrumented carpet findings, a more direct comparison of the two methods is indicated. Stride velocity and stride length appear to be most sensitive to differences between affected and unaffected dogs and to change over time. These data suggest that gait can be assessed as a functionally relevant endpoint in future studies of therapeutics in the XLMTM canine model.

### Funding

This study is supported by the following: Association Française contre les Myopathies (France) to A.B.-B. and M.K.C.; Muscular

Dystrophy Association (United States) GTS36174 to M.K.C. and MDA2 01302 to A.H.B.; Myotubular Trust (UK) to A.B.-B.; Genopole d'Evry (France) to A.B.-B.; National Institutes of Health grants R21AR064503 and R01HL115001 to M.K.C. and R01AR044345 to A.H.B.; Anderson Family Foundation to A.H.B.; and Joshua Frase Foundation to A.H.B. and M.K.C.; Where There's a Will There's a Cure to M.K.C. and the Peter Khuri Myopathy Research Foundation to M.K.C.

### Conflict of interest

There is no conflict of interest.

### Acknowledgments

We thank M. Holder, K. Block, K. Spiller-Poppante, M. Hitchcock, M. Lockard, B. Rider, and K. Poulard for help with the experiments.

### Appendix A. Supplementary data

Supplementary data to this article can be found online at <http://dx.doi.org/10.1016/j.jns.2014.08.032>.

## References

- [1] Jungbluth H, Wallgren-Petersson C, Laporte J. Centronuclear (myotubular) myopathy. *Orphanet J Rare Dis* 2008;3:26.
- [2] Pierson CR, et al. X-linked myotubular and centronuclear myopathies. *J Neuropathol Exp Neurol* 2005;64(7):555–64.
- [3] Heckmatt JZ, et al. Congenital centronuclear (myotubular) myopathy. A clinical, pathological and genetic study in eight children. *Brain* 1985;108(Pt 4):941–64.
- [4] Herman GE, et al. Medical complications in long-term survivors with X-linked myotubular myopathy. *J Pediatr* 1999;134(2):206–14.
- [5] Laporte J, et al. A gene mutated in X-linked myotubular myopathy defines a new putative tyrosine phosphatase family conserved in yeast. *Nat Genet* 1996;13(2):175–82.
- [6] Lawlor MW, et al. Enzyme replacement therapy rescues weakness and improves muscle pathology in mice with X-linked myotubular myopathy. *Hum Mol Genet* 2013;22(8):1525–38.
- [7] Buj-Bello A, et al. AAV-mediated intramuscular delivery of myotubularin corrects the myotubular myopathy phenotype in targeted murine muscle and suggests a function in plasma membrane homeostasis. *Hum Mol Genet* 2008;17(14):2132–43.
- [8] Dowling JJ, et al. Loss of myotubularin function results in T-tubule disorganization in zebrafish and human myotubular myopathy. *PLoS Genet* 2009;5(2):e1000372.
- [9] Buj-Bello A, et al. The lipid phosphatase myotubularin is essential for skeletal muscle maintenance but not for myogenesis in mice. *Proc Natl Acad Sci U S A* 2002;99(23):15060–5.
- [10] Childers MK, et al. Gene therapy prolongs survival and restores function in murine and canine models of myotubular myopathy. *Sci Transl Med* 2014;6(220):220ra10.
- [11] Vainzof M, et al. Animal models for genetic neuromuscular diseases. *J Mol Neurosci* 2008;34(3):241–8.
- [12] Beggs AH, et al. MTM1 mutation associated with X-linked myotubular myopathy in Labrador Retrievers. *Proc Natl Acad Sci U S A* 2010;107(33):14697–702.
- [13] Grange RW, et al. Muscle function in a canine model of X-linked myotubular myopathy. *Muscle Nerve* 2012;46(4):588–91.
- [14] Reuben DB, et al. Motor assessment using the NIH toolbox. *Neurology* 2013;80(11 Suppl. 3):S65–75.
- [15] van der Krogt MM, Delp SL, Schwartz MH. How robust is human gait to muscle weakness? *Gait Posture* 2012;36(1):113–9.
- [16] Scott OM, et al. Quantitation of muscle function in children: a prospective study in Duchenne muscular dystrophy. *Muscle Nerve* 1982;5(4):291–301.
- [17] Davis RB. Reflections on clinical gait analysis. *J Electromyogr Kinesiol* 1997;7(4):251–7.
- [18] Whittle MW. Clinical gait analysis: a review. *Hum Mov Sci* 1996;15(3):369–87.
- [19] Marsh AP, et al. Kinematics of gait in golden retriever muscular dystrophy. *Neuromuscul Disord* 2010;20(1):16–20.
- [20] Light VA, et al. Temporal–spatial gait analysis by use of a portable walkway system in healthy Labrador Retrievers at a walk. *Am J Vet Res* 2010;71(9):997–1002.
- [21] Grange RW, et al. Muscle function in a canine model of X-linked myotubular myopathy. *Muscle Nerve* 2012;46(4):588–91.
- [22] World Health Organization. International classification of functioning, disability, and health: children & youth version: ICF-CY, xxvii. Geneva: World Health Organization; 2007 [322 pp.].
- [23] Bendixen RM, et al. Participation in daily life activities and its relationship to strength and functional measures in boys with Duchenne muscular dystrophy. *Disabil Rehabil* 2014. <http://dx.doi.org/10.3109/09638288.2014.883444>.
- [24] McDonald CM, et al. Relationship between clinical outcome measures and parent proxy reports of health-related quality of life in ambulatory children with Duchenne muscular dystrophy. *J Child Neurol* 2010;25(9):1130–44.
- [25] Henricson E, et al. The 6-minute walk test and person-reported outcomes in boys with Duchenne muscular dystrophy and typically developing controls: longitudinal comparisons and clinically-meaningful changes over one year. *PLoS Curr* 2013:5.
- [26] Carter GT. Ambulation in adults with central neurologic disorders. Foreword. *Phys Med Rehabil Clin N Am* 2013;24(2):xi–xiii.
- [27] Shin JH, et al. Quantitative phenotyping of Duchenne muscular dystrophy dogs by comprehensive gait analysis and overnight activity monitoring. *PLoS ONE* 2013;8(3):e59875.
- [28] Fischmann A, et al. Quantitative MRI and loss of free ambulation in Duchenne muscular dystrophy. *J Neurol* 2013;260(4):969–74.
- [29] Tiffreau V, et al. Gait abnormalities in type 1 myotonic muscular dystrophy: 3D motion analysis, energy cost and surface EMG. *Comput Methods Biomech Biomed Engin* 2012;15(Suppl. 1):171–2.
- [30] Galli M, et al. Gait pattern in myotonic dystrophy (Steinert disease): a kinematic, kinetic and EMG evaluation using 3D gait analysis. *J Neurol Sci* 2012;314(1–2):83–7.
- [31] Ganea R, et al. Gait assessment in children with Duchenne muscular dystrophy during long-distance walking. *J Child Neurol* 2012;27(1):30–8.
- [32] Esser P, et al. Assessment of spatio-temporal gait parameters using inertial measurement units in neurological populations. *Gait Posture* 2011;34(4):558–60.
- [33] McDonald CM, et al. The 6-minute walk test in Duchenne/Becker muscular dystrophy: longitudinal observations. *Muscle Nerve* 2010;42(6):966–74.
- [34] Gaudreault N, et al. Gait patterns comparison of children with Duchenne muscular dystrophy to those of control subjects considering the effect of gait velocity. *Gait Posture* 2010;32(3):342–7.
- [35] Sienko Thomas S, et al. Classification of the gait patterns of boys with Duchenne muscular dystrophy and their relationship to function. *J Child Neurol* 2010;25(9):1103–9.
- [36] Barthelemy I, et al. Effects of an immunosuppressive treatment in the GRMD dog model of Duchenne muscular dystrophy. *PLoS ONE* 2012;7(11):e48478.
- [37] Barthelemy I, et al. Longitudinal ambulatory measurements of gait abnormality in dystrophin-deficient dogs. *BMC Musculoskelet Disord* 2011;12:75.
- [38] Barthelemy I, et al. Gait analysis using accelerometry in dystrophin-deficient dogs. *Neuromuscul Disord* 2009;19(11):788–96.
- [39] Shimatsu Y, et al. Major clinical and histopathological characteristics of canine X-linked muscular dystrophy in Japan, CXMDJ. *Acta Myol* 2005;24(2):145–54.
- [40] Shelton GD, et al. Muscular dystrophy in female dogs. *J Vet Intern Med* 2001;15(3):240–4.
- [41] Goddard MA, et al. Establishing clinical end points of respiratory function in large animals for clinical translation. *Phys Med Rehabil Clin N Am* 2012;23(1):75–94 xi.